Article

# Monumental architecture at Aguada Fénix and the rise of Maya civilization

https://doi.org/10.1038/s41586-020-2343-4

Received: 26 November 2019

Accepted: 30 April 2020

Published online: 03 June 2020

Check for updates

Takeshi Inomata[1]✉, Daniela Triadan[1], Verónica A. Vázquez López[2], Juan Carlos Fernandez-Diaz[3], Takayuki Omori[4], María Belén Méndez Bauer[5], Melina García Hernández[6], Timothy Beach[7], Clarissa Cagnato[8], Kazuo Aoyama[9] & Hiroo Nasu[10]

Archaeologists have traditionally thought that the development of Maya civilization was gradual, assuming that small villages began to emerge during the Middle Preclassic period (1000–350 BC; dates are calibrated throughout) along with the use of ceramics and the adoption of sedentism[1]. Recent finds of early ceremonial complexes are beginning to challenge this model. Here we describe an airborne lidar survey and excavations of the previously unknown site of Aguada Fénix (Tabasco, Mexico) with an artificial plateau, which measures 1,400 m in length and 10 to 15 m in height and has 9 causeways radiating out from it. We dated this construction to between 1000 and 800 BC using a Bayesian analysis of radiocarbon dates. To our knowledge, this is the oldest monumental construction ever found in the Maya area and the largest in the entire pre-Hispanic history of the region. Although the site exhibits some similarities to the earlier Olmec centre of San Lorenzo, the community of Aguada Fénix probably did not have marked social inequality comparable to that of San Lorenzo. Aguada Fénix and other ceremonial complexes of the same period suggest the importance of communal work in the initial development of Maya civilization.

The period around 1200–1000 BC was a critical time of social change in the Maya lowlands. Prior to this period, the inhabitants of this area did not use ceramics and probably maintained mobile ways of life by combining hunting, gathering and fishing with the cultivation of maize and other crops[2]. They began to adopt ceramics and greater degrees of sedentism at the beginning of the Middle Preclassic period, and researchers have long thought that ceremonial centres with large pyramids did not develop until late in the Middle Preclassic period, or in the Late Preclassic and Terminal Preclassic periods (hereafter, Late–Terminal Preclassic) (350 BC–AD 250). However, the discovery of a formal ceremonial complex and an artificial plateau at Ceibal dating to 950 BC suggests that substantial ceremonial centres developed in the Maya lowlands earlier than was previously thought[3,4]. Here, the term artificial plateau refers to horizontal buildings larger than 200 × 200 m, as distinguished from smaller supporting platforms. A few centuries later, other centres in the Maya lowlands—such as Cival, Komchen, Nakbe, Yaxnohcah and Xocnaceh—also built artificial plateaus or large platforms[5–9]. Our research in Tabasco (Mexico) has revealed an even older and larger ceremonial centre, Aguada Fénix (Extended Data Fig. 1).

We began the Middle Usumacinta Archaeological Project in the area along the Usumacinta and San Pedro Rivers in Tabasco in 2017 (Fig. 1). Despite previous investigations[10,11] in the area, the Preclassic period of this region was poorly understood. We thought that this area, located at the western periphery of the Maya lowlands, might hold the key to understanding the relationship between the Olmec civilization and Maya society. The Olmec centre of San Lorenzo—which reached its heyday between 1400 and 1150 BC—is characterized by an enormous artificial plateau and colossal sculptures of stone heads, but does not have pyramids[12,13]. During the Middle Preclassic period (possibly after 800 BC), La Venta became a dominant Olmec centre, containing a large pyramid and mounds[14–16]. Archaeologists have long debated whether the inhabitants of the Maya lowlands inherited the legacy of San Lorenzo, and whether they received direct influence from La Venta[17,18].

## Survey and excavation

A high-resolution lidar survey conducted by the National Center for Airborne Laser Mapping (NCALM) and a low-resolution lidar survey by the Instituto Nacional de Estadística y Geografía (INEGI) in our study area revealed 21 ceremonial centres in a standardized spatial configuration, which we call the Middle Formative Usumacinta (MFU) pattern. The MFU pattern is characterized by a rectangular shape defined by rows of low mounds, oriented roughly north–south (Fig. 2). At the centre of each MFU complex is a so-called E-group assemblage, which consists of a round or square western mound and an elongated eastern platform. Many other sites in the Maya lowlands that date to the Middle Preclassic

[1]School of Anthropology, University of Arizona, Tucson, AZ, USA. [2]Department of Anthropology and Archaeology, University of Calgary, Alberta, Canada. [3]National Center for Airborne Laser Mapping (NCALM), University of Houston, Houston, TX, USA. [4]University Museum, University of Tokyo, Tokyo, Japan. [5]Estudios Mesoamericanos, Universidad Nacional Autónoma de México, Mexico City, Mexico. [6]Middle Usumacinta Archaeological Project, Balancán, Mexico. [7]Department of Geography and the Environment, University of Texas, Austin, TX, USA. [8]UMR 8096, Archéologie des Amériques, Nanterre, France. [9]Faculty of Humanities, Ibaraki University, Mito, Japan. [10]Faculty of Biosphere-Geosphere Science, Okayama University of Science, Okayama, Japan. ✉e-mail: inomata@arizona.edu

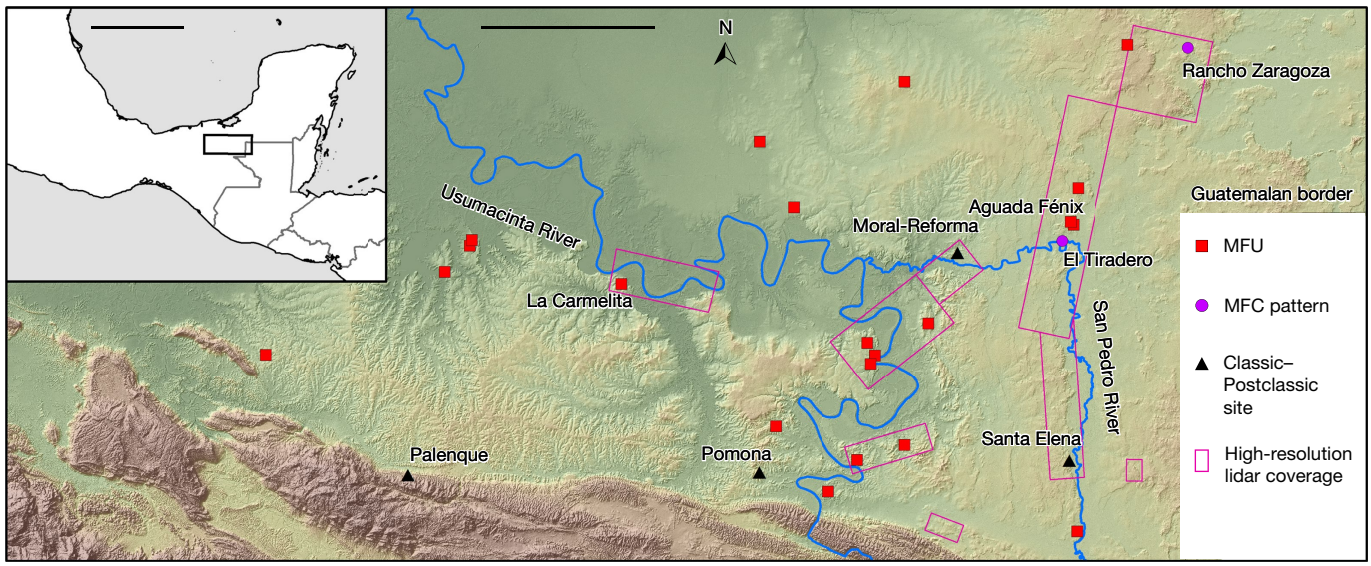


**Fig. 1 | Map of the Middle Usumacinta region.** The low-resolution INEGI lidar covers the entire region. MFC, Middle Formative Chiapas. Map topographic data are from the INEGI lidar survey (www.inegi.org.mx). Scale bars, 25 km (main panel), 400 km (inset).

and Late–Terminal Preclassic periods have E-group assemblages, but no rectangular site plans are found to the east of our study area[19]. We also found smaller versions of the MFU complex—measuring less than 400 m in length—that we call 'minor MFU' complexes. Moreover, there are roughly rectangular complexes that exhibit less formal shapes, without a clear E-group assemblage.

The MFU pattern is probably related to what has previously been referred to as the Middle Formative Chiapas pattern, which is found at sites of the Middle Preclassic period (including La Venta, centres in the Grijalva River basin, Tzutzuculi and Ceibal)[17,20]. The Middle Formative Chiapas pattern consists of an E-group assemblage and large platforms that are arranged along a north–south axis, but lacks the delineated rectangular shape of the MFU pattern. Middle Formative Chiapas complexes appear to have been built between 1000 and 350 BC. Excavations at the Middle Formative Chiapas centres of La Venta, San Isidro, Chiapa de Corzo and Ceibal have unearthed a series of caches with greenstone axes: these communities probably shared similar ritual concepts and practices[14,21–23].

The largest of the MFU sites in our study region is Aguada Fénix (Fig. 1). The high-resolution lidar shows that the main plateau of this site has a rectangular form, measuring 1,413 m from north to south and 399 m from east to west, and that its edges were lined with low platforms. Square wings attached to the eastern and western sides of this plateau give it a narrow cruciform-like overall shape (Fig. 2). The large southwest platform may have been added later to this original form. Unlike other MFU sites (which do not have substantial build-ups of plaza areas), this construction rises 10 to 15 m above the surrounding ground surface. This site was not known before our research, probably because a horizontal construction on this scale is difficult to recognize from the ground level. A large E-group assemblage, with the eastern platform measuring 401 m in length, occupies the centre of the formation. The plateau is surrounded by one MFU complex, five minor MFU complexes, multiple rectangular complexes and artificial reservoirs, as well as by wetlands on the east. In addition, nine causeways extend from the plateau. The northern and southern causeways are connected to the plateau by large ramps. The northwest causeway is the longest of all and extends 6.3 km, connecting multiple complexes along the way (Extended Data Fig. 2). The west plateau is another large construction, measuring 390 × 270 m horizontally and 15–18 m in height; it stands 1.7 km to the west of the main plateau.

Our excavation results indicate that the main plateau was raised multiple times with clay and earth fills, and reached a size close to the current one around 800 BC. In the 7.5-m-deep operation NR3A (for definitions of excavation designations, see 'Excavation' in Methods), we uncovered a dense deposit of ceramics, bones and shells covering bedrock, which appears to predate the construction of the plateau (Extended Data Figs. 3, 4). The plateau construction events included two episodes, in which clays and other soils of various colour were placed in multiple layers, each layer forming checkerboard-like horizontal patterns (Extended Data Fig. 5). The presence of similar—albeit thinner—fills in operations NR5A, NR7A and NR9A indicates that the builders placed elaborate fills of multiple colours over a large part of the plateau, which they covered with a floor at the end of each construction event.

The results from operation NR7A showed that this edge platform was also constructed mostly with earthen fills during the Middle Preclassic period. Nevertheless, four structures located directly west of the E group have walls made of roughly shaped megalithic blocks (Extended Data Fig. 6). Operation NR8A revealed blocks measuring up to 3.0 × 1.0 × 0.7 m. Through excavations in two of the causeways (operations NR4A and NR6A), we also confirmed that these wide streets were built during the Middle Preclassic period, with fill thicknesses of around 2.6 m.

## Radiocarbon dates

We obtained 69 radiocarbon dates, which we analysed using Bayesian statistics (Extended Data Fig. 7, Supplementary Methods, Supplementary Data, Supplementary Table 1). Charcoal samples from the earliest deposits in operations NR3A and NR7A at Aguada Fénix yielded dates of around 1250–1150 BC and 1150–1050 BC, respectively. These data indicate that the people of this region had begun to use ceramics by 1200 BC, one to two centuries earlier than those of Ceibal, Tikal, Cahal Pech, Cuello and other Maya communities[2]. Plateau construction began by 1000 BC if not earlier, slightly before the initial construction of the ceremonial complex at Ceibal. However, construction activity at Aguada Fénix ceased soon after 800 BC. Carbon samples from two of the causeways yielded radiocarbon dates of 950–800 BC. In addition, samples taken from test excavations in areas around the plateau, where residences may have existed, returned dates of 1000–750 BC. At the MFU site of La Carmelita, carbon samples from the lowest layer yielded dates of around 900 BC, and samples from the upper layers gave dates of around 750 BC (Extended Data Fig. 8). We suspect that other

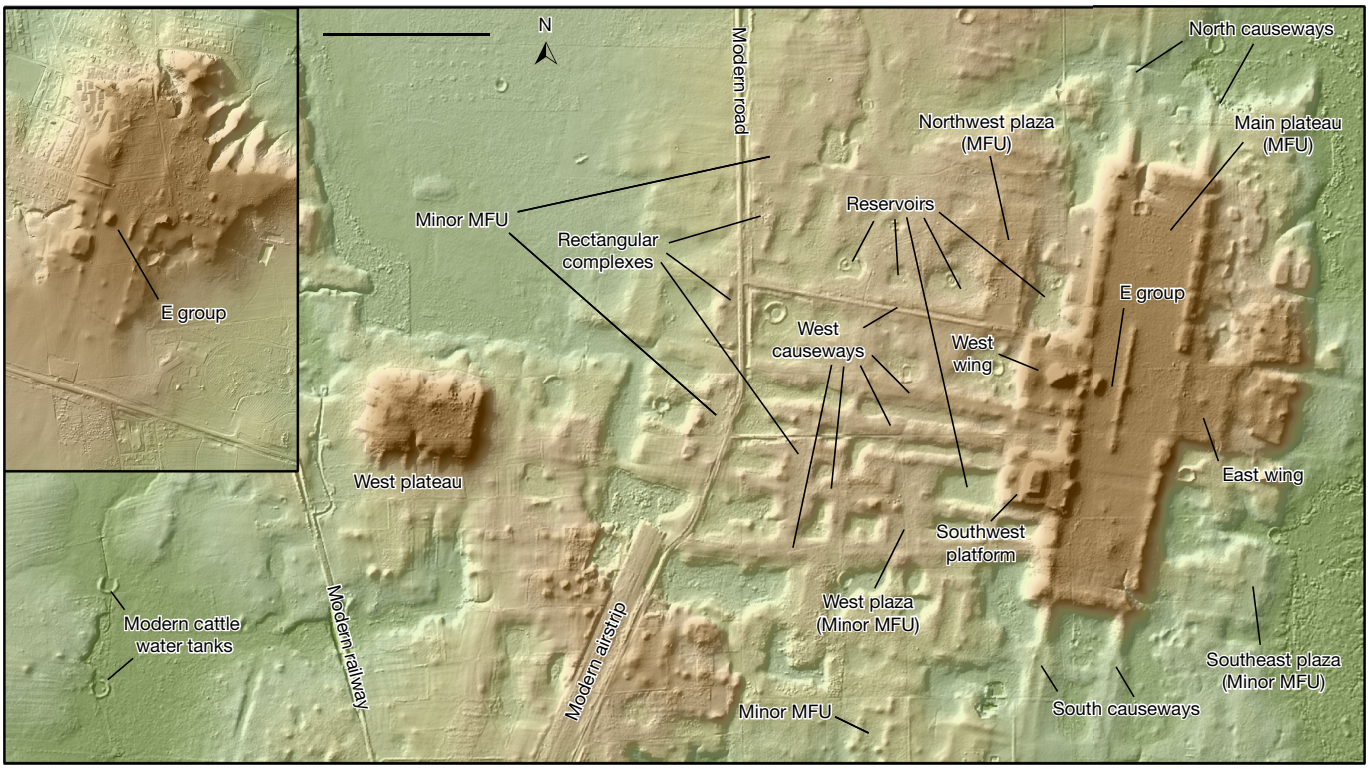


**Fig. 2 | High-resolution lidar images of Aguada Fénix and La Carmelita.** Main panel, Aguada Fénix; inset, La Carmelita. Scale bar, 500 m (both images are on the same scale).

MFU sites in the region were also built during the period between 1000 and 750 BC. Aguada Fénix and other MFU sites appear to have been abandoned by 750 BC. Small groups returned to Aguada Fénix during the Late–Terminal Preclassic and Late Classic periods.

## Volume estimates

In addition to the excavations, we conducted auger tests in the main and west plateaus at Aguada Fénix to estimate their construction volumes. The results suggest that the builders constructed the main plateau over a natural rise of bedrock (Extended Data Fig. 9a, Supplementary Table 2). On the basis of the reconstructed bedrock surface and lidar data, we estimate the fill volume for the Middle Preclassic portion of the main plateau at 3,200,000–4,300,000 $m^3$. We calculate that this Middle Preclassic construction required 10,000,000–13,000,000 person-days (Extended Data Fig. 9b).

The volume of the main plateau surpasses that of the La Danta complex at the Late–Terminal Preclassic centre of El Mirador, the largest construction previously known in the Maya lowlands[7] (Extended Data Fig. 9c). Pyramids built during the Classic period in the Maya lowlands are substantially smaller[24]. In other words, the main plateau of Aguada Fénix is the largest construction in the pre-Hispanic Maya area. The volume of the plateau at San Lorenzo is larger but after the decline of this Olmec centre, Aguada Fénix represented the largest construction effort during the Middle Preclassic and Late–Terminal Preclassic periods in Mesoamerica[13]. It is noteworthy that this enormous construction at Aguada Fénix was built in a short span, of roughly 200 years.

## Discussion

Artificial plateaus may be characterized as horizontal monumentality, which contrasts with the vertical dimensions of pyramids. The construction of the plateaus at Aguada Fénix most probably followed the tradition established at San Lorenzo. The builders combined this legacy of the previous era with elements that emerged after the decline of San Lorenzo, including standardized site plans, the E-group assemblage and other pyramidal constructions. These innovations probably occurred through intensive interregional interaction. The Pacific coast may have been an important area for the development of pyramidal structures[25,26]. Aguada Fénix and other MFU complexes shared standardized spatial configurations and the E-group assemblage with the Middle Formative Chiapas centres in the Grijalva River region. A greenstone axe cache found in the E-group plaza of Aguada Fénix indicates that its inhabitants also practiced rituals similar to those of La Venta, the Grijalva River region and Ceibal (Extended Data Fig. 10). Aguada Fénix appears to have had a central role in this dynamic process of social and cultural innovation between 1100 and 800 BC.

Despite their architectural and ritual commonality, the political and cultural settings of these regions were diverse. The ceramics found at Aguada Fénix resemble the Real ceramics from Ceibal and are markedly different from those of the La Venta or the Grijalva River region. Although the ceramics do not necessarily indicate that the builders of Aguada Fénix were speakers of a Mayan language, they appear to have had closer cultural affinities with the Maya lowlands than with the Olmec area. This interpretation is bolstered by the observation that all analysed obsidian pieces from our study area originated from El Chayal and other Guatemalan sources (Supplementary Table 3). This finding contrasts with the pattern at San Lorenzo, where a substantial portion of obsidian was imported from Mexican sources[27]. It is also likely that social inequality at Aguada Fénix was not as pronounced as at San Lorenzo and La Venta. Unlike those Olmec centres, Aguada Fénix does not exhibit clear indicators of marked social inequality, such as sculptures representing high-status individuals. The only stone sculpture found so far at Aguada Fénix depicts an animal (Extended Data Fig. 10). If these interpretations are correct, they imply that the Gulf Coast Olmec region was not the only centre of cultural development and that innovations did not always emanate from the most hierarchical polities.

An important factor for the emergence of Aguada Fénix and related sites may have been the transition from a mobile lifeway to sedentism, stimulated by a heavier reliance on maize agriculture[2,28–31]. The scarcity of residential platforms around many of the MFU sites suggests that a substantial portion of the inhabitants of the Middle Usumacinta region maintained a degree of residential mobility. At the same time, results from the analysis of starch grains found on grinding stones are consistent with the assumption that the use of maize was common during the period of plateau construction (Supplementary Table 4). Under rapidly changing social conditions, many inhabitants of the region may have actively participated in the transformation of the lived landscape to create new places of gathering without coercion from powerful elites. Although the tradition of horizontal monumentality was first established at the hierarchical polity of San Lorenzo, the inclusive forms of plateaus may have been appealing to communities without marked social inequality. With the development of more hierarchical organization, later sites—including La Venta, Takalik Abaj, Nakbe and Tikal—emphasized tall pyramids, access to which was possibly restricted to a privileged few.

Aguada Fénix may be analogous to early ceremonial constructions that emerged during pre-agricultural or incipient agricultural periods in other parts of the world, including the Near East, the Andes and the American Southeast[32–36]. However, Aguada Fénix is different from these examples in that Mesoamerican groups had domesticated maize and other crops several millennia before the rise of Aguada Fénix[37]. These observations urge us to explore the diverse processes that existed in the construction of monumental structures in societies with limited social inequality.

## Online content

Any methods, additional references, Nature Research reporting summaries, source data, extended data, supplementary information, acknowledgements, peer review information; details of author contributions and competing interests; and statements of data and code availability are available at https://doi.org/10.1038/s41586-020-2343-4.


1. Adams, R. E. W. *The Origins of Maya Civilization* (Univ. New Mexico Press, 1977).
2. Lohse, J. C. Archaic origins of the lowland Maya. *Lat. Am. Antiq.* **21**, 312–352 (2010).
3. Inomata, T., Triadan, D., Aoyama, K., Castillo, V. & Yonenobu, H. Early ceremonial constructions at Ceibal, Guatemala, and the origins of lowland Maya civilization. *Science* **340**, 467–471 (2013).
4. Inomata, T., Triadan, D., Pinzón, F. & Aoyama, K. Artificial plateau construction during the Preclassic period at the Maya site of Ceibal, Guatemala. *PLoS ONE* **14**, e0221943 (2019).
5. Estrada-Belli, F. in *Early New World Monumentality* (eds Burger, R. L. & Rosenswig, R. M.) 198–230 (Univ. Press Florida, 2012).
6. Andrews, E. W. V, Bey, G. J. III & Gunn, C. M. in *Pathways to Complexity: A View from the Maya Lowlands* (eds Brown, M. K. & Bey, G. J. III) 49–86 (Univ. Press Florida, 2018).
7. Hansen, R. D. & Suyuc, L. E. *Mirador* (FARES Guatemala, 2016).
8. Gallareta Negrón, T. in *Pathways to Complexity: A View from the Maya Lowlands* (eds Brown, M. K. & Bey, G. J. III) 276–291 (Univ. Press Florida, 2018).
9. Reese-Taylor, K. in *Maya E Groups: Calendars, Astronomy, and Urbanism in the Early Lowlands* (eds Freidel, D. A. et al.) 480–513 (Univ. Press Florida, 2017).
10. Rands, R. L. in *Origins of Maya Civilization* (ed. Adams, R. E. W.) 159–180 (Univ. New Mexico Press, 1977).
11. Ochoa, L. in *Antropología e Historia de los Mixe-Zoques y Mayas: Homenaje a Frans Blom* (eds Ochoa, L. & Lee, T. A.) 147–174 (Instituto de Investigaciones Filológicas, UNAM, 1983).
12. Coe, M. D. & Diehl, R. A. *In the Land of the Olmec* (Univ. Texas Press, 1980).
13. Cyphers, A. in *The Origins of Maya States* (eds Traxler, L. P. & Sharer, R. J.) 83–122 (Univ. Pennsylvania Museum of Archaeology and Anthropology, 2016).
14. Drucker, P., Heizer, R. F. & Squier, R. H. *Excavations at La Venta, Tabasco, 1955* (Smithsonian Institution, 1959).
15. González Lauck, R. B. in *The Place of Stone Monuments: Context, Use, and Meaning in Mesoamerica's Preclassic Tradition* (eds Guernsey, J. et al.) 177–205 (Dumbarton Oaks Research Library and Collection, 2010).
16. Clark, J. E. in *The Origins of Maya States* (eds Traxler, L. P. & Sharer, R. J.) 123–224 (Univ. Pennsylvania Museum of Archaeology and Anthropology, 2016).
17. Clark, J. E. & Hansen, R. D. in *Royal Courts of the Ancient Maya, Volume 2: Data and Case Studies* (eds Inomata, T. & Houston, S. D.) 1–45 (Westview Press, 2001).
18. Estrada-Belli, F. *The First Maya Civilization: Ritual and Power before the Classic Period* (Routledge, 2011).
19. Freidel, D. A., Chase, A. F., Dowd, A. S. & Murdock, J. *Maya E Groups: Calendars, Astronomy, and Urbanism in the Early Lowlands* (Univ. Press Florida, 2017).
20. Lowe, G. W. in *The Origins of Maya Civilization* (ed. Adams, R. E. W.) 197–248 (Univ. New Mexico Press, 1977).
21. Lowe, G. W. in *The Olmec and their Neighbors* (eds Coe, M. D. & Grove, D.) 231–256 (Dumbarton Oaks Research Library and Collection, 1981).
22. Bachand, B. R. & Lowe, L. S. in *Arqueología Reciente de Chiapas: Contribuciones del Encuentro Celebrado en el 60° Aniversario de la Fundación Arqueológica Nuevo Mundo* (eds Lowe, L. S. & Pye, M. E.) 45–68 (Brigham Young Univ., 2012).
23. Inomata, T. & Triadan, D. Middle Preclassic Caches from Ceibal, Guatemala. *Maya Archaeol.* **3**, 56–91 (2016).
24. Webster, D. & Kirker, J. Too many Maya, too few buildings: investigating construction potential at Copán, Honduras. *J. Anthropol. Res.* **51**, 363–387 (1995).
25. Hodgson, J. G., Clark, J. G. & Gallaga Murrieta, E. Ojo de Agua monument 3: a new Olmec-style sculpture from Ojo de Agua, Chiapas, Mexico. *Mexicon* **32**, 139–144 (2010).
26. Love, M. & Guernsey, J. in *Early Mesoamerican Social Transformations: Archaic and Formative Lifeways in the Soconusco Region* (ed. Lesure, R. G.) 170–188 (Univ. California Press, 2011).
27. Hirth, K., Cyphers, A., Cobean, R., De León, J. & Glascock, M. D. Early Olmec obsidian trade and economic organization at San Lorenzo. *J. Archaeol. Sci.* **40**, 2784–2798 (2013).
28. Blake, M., Clark, J. E., Voorhies, B., Love, M. W. & Chisholm, B. S. Prehistoric subsistence in the Soconusco region. *Curr. Anthropol.* **33**, 83–94 (1992).
29. Clark, J. E., Pye, M. E. & Gosser, D. C. in *Archaeology, Art, and Ethnogenesis in Mesoamerican Prehistory: Papers in Honor of Gareth W. Lowe* (eds Lowe, L. S. & Pye, M. E.) 23–42 (Brigham Young Univ., 2007).
30. Inomata, T. et al. Development of sedentary communities in the Maya lowlands: coexisting mobile groups and public ceremonies at Ceibal, Guatemala. *Proc. Natl Acad. Sci. USA* **112**, 4268–4273 (2015).
31. Rosenswig, R. M. in *Early Mesoamerican Social Transformations: Archaic and Formative Lifeways in the Soconusco Region* (ed. Lesure, R. G.) 242–271 (Univ. California Press, 2011).
32. Schmidt, K. Göbekli Tepe–the Stone Age sanctuaries: new results of ongoing excavations with a special focus on sculptures and high reliefs. *Documenta Praehistorica* **37**, 239–255 (2010).
33. Solis, R. S., Haas, J. & Creamer, W. Dating Caral, a preceramic site in the Supe Valley on the central coast of Peru. *Science* **292**, 723–726 (2001).
34. Saunders, J. W. et al. Watson Brake, a Middle Archaic mound complex in northeast Louisiana. *Am. Antiq.* **70**, 631–668 (2005).
35. Stanish, C. *The Evolution of Human Co-Operation: Ritual and Social Complexity in Stateless Societies* (Cambridge Univ. Press, 2017).
36. Burger, R. L. & Rosenswig, R. M. *Early New World Monumentality* (eds Burger, R. L. & Rosenswig, R. M.) (Univ. Press Florida, 2012).
37. Piperno, D. R., Ranere, A. J., Holst, I., Iriarte, J. & Dickau, R. Starch grain and phytolith evidence for early ninth millennium B.P. maize from the Central Balsas River Valley, Mexico. *Proc. Natl Acad. Sci. USA* **106**, 5019–5024 (2009).

# Methods

## Lidar

Lidar data are now commonly used in archaeological investigations in southern Mesoamerica, as well as in other tropical regions of the world[38–51]. In our research, the high-resolution lidar data were obtained by NCALM. The NCALM crew collected lidar data for 109 $km^2$ on 6 May 2017. After the discovery of Aguada Fénix, we acquired additional lidar data for a nominal area of 745 $km^2$ between 9 June 2019 and 17 June 2019. The site of La Carmelita was surveyed in the 2017 NCALM campaign, and the entire extent of Aguada Fénix was covered by the NCALM high-resolution lidar data of 2019.

For both campaigns, the NCALM team used an Optech Titan lidar system, which is equipped with three channels of laser at wavelengths of 1,550, 1,064 and 532 nm[52,53]. The following parameters were used for the 2019 survey: a flying height of 650 m above ground level; a pulse repetition frequency of 150 kHz; a scan frequency of 25 Hz; and a scan angle of ±30°. This configuration produced swath widths of 750 m, which were laterally overlapped by 50%, with a flight line spacing of 345 m. Assessed over a 298.2-$km^2$ section of the 2019 survey and 10-m pixels, these settings yielded densities of 14.7 pulses per $m^2$, 18.5 returns per $m^2$ and 10.4 ground returns per $m^2$. To assess the precision of the lidar height model, the NCALM crew compared the lidar data against 965 kinematic GPS measurements processed with differential and dual wavelength geodetic techniques. The results indicate that the precision of the lidar models is within ±1.9 cm (1 s.d.) of the GPS measurements. NCALM researchers classified laser points using TerraScan software, and created a digital elevation model (DEM; a bare-earth model without vegetation and modern buildings) and a digital first surface model (including vegetation and buildings) at a horizontal spacing of 1 m for the 2017 data and 0.5 m for the 2019 data. NCALM researchers delivered the DEM and digital first surface model to the archaeologists in ESRI .flt raster format, and delivered the point cloud data in LAS format.

The examination of point clouds indicates that the high-resolution lidar used by NCALM penetrated the dense canopies of high secondary vegetation. However, where there is dense vegetation close to the ground surface (vegetation shorter than 2m (such as dense undergrowth, dense, low secondary vegetation and dense grass)), there may be mixed returns with the signals of both vegetation and the terrain. The results of our field validation suggest that, under these conditions, subtle archaeological features may be difficult to detect, but structures higher than 1.5 m can be identified in the DEM derived from the high-resolution lidar[54–56]. Most parts of our study area are covered by pasture, mature secondary vegetation or tree plantations. In these areas, low mounds and platforms—measuring 0.2 to 0.5 m in height—can usually be detected in the high-resolution lidar.

The low-resolution lidar data were collected by the INEGI (a Mexican government agency) in 2012. These data were intended for diverse uses by the Mexican government, industries, researchers of various fields and the general public. The INEGI used a Leica Geosystems ALS50-II lidar system and produced DEMs and digital first surface models at a horizontal spacing of 5 m, which are publicly available through the INEGI website (www.inegi.org.mx). The INEGI does not publish the parameters used for the acquisition of lidar data, but the laser point density appears to be generally low. We began to analyse these publicly available data in 2017. Our analysis shows that the INEGI DEMs often do not represent details of the ground topography well in forested areas. Substantial parts of our study areas, however, are deforested and used as pastures. The low-resolution INEGI lidar images show many of the large archaeological features under these conditions[57].

To examine the distribution of archaeological sites, we analysed the NCALM and INEGI lidar data using ArcGIS. We applied various visualization techniques, including hillshades, principal component analysis of multi-directional hillshades, slope gradient, sky view factor analysis, simple local relief models and red relief image map[56,58–65].

The field validation of archaeological sites is ongoing. We have visited 42 areas, which were all confirmed to be archaeological sites. In addition to Aguada Fénix and La Carmelita, five sites (Buenavista, El Macabil, El Saraguato, Rancho Zaragoza and Chrisóforo Chiñas) have been confirmed to have the MFU pattern.

## Excavation

Excavations followed methods established during the investigation of Ceibal[66]. To control the proveniences of artefacts, we use a hierarchical recording system of excavation contexts, consisting of (from largest to smallest division) site code, operation, suboperation, unit, level and lot. The site codes consist of two letters: NR for the central part of Aguada Fénix; AF for peripheral areas of Aguada Fénix; LC for La Carmelita; TR for El Tiradero; and ZR for Rancho Zaragoza. An operation refers to the excavation of a mound group or a similar area; a suboperation refers to the excavation of individual structures or a small area; a unit is a horizontal division, usually of 2 × 2 m; a level is a major group of stratigraphic layers; and a lot is any natural or arbitrary division within a unit and a level. We screened all excavated soils with 1/4-inch (or smaller) mesh. We collected soil samples for floatation from important contexts (such as middens), in which we collected both floated organic materials and heavy fractions.

Middle Preclassic fills of the Aguada Fénix main plateau consisted mostly of dark clay, and floors were made of dark clay or lighter coloured earth. In operation NR3A, we identified nine Middle Preclassic floors. Thin layers of earthen fills mixed with stones were added over the Middle Preclassic construction during the Late–Terminal Preclassic (350 BC–AD 250) and the Late Classic (AD 600–810) periods. The results of operation NR7A suggest that most platforms placed along the edges of the main plateau were constructed during the Middle Preclassic period—probably before 800 BC—with earthen fills. Operations NR4A and NR6A showed that the south and west causeways were built between 950 and 800 BC with 19 to 25 successive floors, reaching total fill thicknesses of around 2.6 m.

## Ceramic analysis

Because the ceramics of Aguada Fénix and La Carmelita were similar to those from Ceibal, we began our ceramic analysis by applying the ceramic typology of Ceibal[67–69]. We used Ceibal type names (such as Abelino Red, Hueche White and Crisanto Black) for ceramics that exhibited close similarities to those of Ceibal. We gave preliminary type and group names to ceramics unique to the region. They include the Tiradero group, which is characterized by thin buff to white pastes with volcanic ash temper. Some Tiradero vessels have red paint. Only a very small portion of the ceramics appears to have some affinities with materials from the Gulf Coast or Chiapas. We placed those ceramics in temporary categories. We will decide whether we will use type names from the Gulf Coast or Chiapas or whether we give new type names after we conduct thorough comparative studies with materials from other regions. We also conducted modal analysis, particularly focusing on vessel forms. Modal data also helped us to correlate the occupation of the Middle Usumacinta region with ceramic phases of Ceibal and other lowland Maya sites. We have yet to give phase names to the occupation of Aguada Fénix and La Carmelita: we will do so after we obtain more excavation data from various sites in the region.

## Auger tests

We first used a hand-operated bucket auger, following the method used in the Olmec area[70]. However, it was difficult to penetrate through limestone cobbles, which are often present in the upper layers of the Aguada Fénix plateau. We then contracted a mechanical auger, which is generally used for digging wells in the region. We used a Deeprock hydraulic rotary auger DR20, which was equipped with a 4-inch point made of tungsten carbide drill tips and with metal tubes of 2-inch diameter and 5-feet length. The auger was powered by a gasoline motor,

and bored holes of 11-cm diameter. A water pump supplied water to the drill point, which extracted excavated materials. Although it is possible to use compressed air instead of water, this method was substantially more expensive. We thus decided to use the hydraulic auger.

By collecting the materials extracted with the water with a fine mesh, we could gain a general understanding of the stratigraphy as the auger advanced. The auger penetrated soft limestone blocks, but it had difficulty in penetrating hard crystallized carbonate rock or large nodules of chert. The bedrock of the area generally consists of a thin layer of soft, white marl that overlies hard carbonate rock. When the auger reached this sequence of soft and hard materials, we interpreted it as bedrock. When we encountered hard materials at depths shallower than expected, we excavated 1 × 1-m test units to verify whether we had reached bedrock. At auger test 2, we found that the auger was blocked by a large nodule of chert; at auger test 6, we confirmed that bedrock was at a depth of 1.5 m. At auger test 11 (placed on the west plateau), we reached soft, white material at depths of 7.0 and 15.0 m and hard material at 19.5 m, which made the interpretation of stratigraphy difficult.

Our stratigraphic interpretations based on the auger tests are tentative, and need to be verified with future excavations. Nonetheless, these interpretations serve the purpose of avoiding an overestimation of construction volume. Although it was sometimes difficult to determine whether soft, white layers represented the beginning of bedrock or materials included in fills, black clay layers could be reasonably interpreted as construction fills. In other words, there is the possibility that future research could reveal deeper bedrock surfaces (leading to larger estimates of construction volumes), but it is less likely that our current volume estimates become substantially smaller.

**Volume calculation**

Using stratigraphic data obtained from the excavations and the auger tests, we estimated the fill volume of the main plateau of Aguada Fénix. We followed the method that was used in the analysis of the plateau of Ceibal[4]. To summarize in brief, we created a three-dimensional (3D) model of the bedrock, using the Microstation CAD program. We first drew the positions of the bedrock that were found in excavations and auger tests. We then drew areas between them by assuming a smooth surface of the bedrock. For those areas, we made three versions of estimated bedrock positions: (1) the estimate that we think most likely; (2) the highest probable positions; and (3) the lowest probable positions. The 3D data of the bedrock were then imported into ArcGIS. We used the DEM derived from the NCALM high-resolution lidar as an approximation of the final form of the plateau. By subtracting the bedrock model raster files from the DEM raster, we obtained the most likely, high and low estimates of 3,790,000, 4,480,000 and 3,390,000 $m^3$, respectively, for the total plateau fill volume. In many areas of the plateau, we encountered fills dating to the Late–Terminal Preclassic or Classic period that measured 0.1 to 0.5 m in thickness. By using 0.3 m as an average thickness of these later constructions, we estimated the fill volume for the Late–Terminal Preclassic and Classic periods at 160,000 $m^3$. By subtracting this amount from the total estimated volumes, we reached the most likely, high and low estimates of 3,630,000, 4,320,000 and 3,230,000 $m^3$, respectively, for the Middle Preclassic fill volume (Extended Data Fig. 9b).

We determined that the effects of lidar measurement errors on these calculations are minimal, and we did not incorporate them in our volume estimates. The error range of ±1.9 cm in the NCALM lidar height model is negligible compared to the level of uncertainty in the estimates of bedrock positions. In addition, the positions of bedrock in our 3D models were plotted relative to the lidar-derived DEM, and, thus, vertical errors in lidar do not affect volume estimates in any meaningful way. Other potential factors that might affect the volume estimates include: (1) mixed returns of lidar caused by dense, low vegetation; and (2) soil erosion that happened after the abandonment of the site. There are areas of mixed returns around the east wing and the southern end of the plateau. Their total area measures 152,000 $m^2$. Examinations of the DEM and point clouds, as well as observations during a pedestrian survey, suggest that mixed returns may have caused the DEM to be an average of 0.1 m higher than the real ground surface in those areas. These errors may have increased a plateau volume estimate by 15,200 $m^3$, which is a fairly small effect. We do not have data with which to assess the quantity of soil erosion. We simply assumed that the volume loss caused by soil erosion offsets the addition by mixed returns of lidar.

The west plateau was explored with only one auger test, and its construction sequence is not clear. The auger reached possible bedrock, consisting of soft limestone or marl, at depths of 7.0 m and 15.0 m. It also hit hard rock at a depth of 19.5 m. However, this level is lower than the current surrounding ground surface, and we suspect that it is below the bedrock surface. If the bedrock surface is at 7.0 m, the volume of the west plateau would be roughly 600,000 $m^3$. Alternatively, the depth of 15.0 m would indicate a volume of 1,100,000 $m^3$.

Although calculations of volumes can contain substantial margins of error, the estimates for the main plateau are considerably larger than the volume of 2,800,000 $m^3$ estimated for the La Danta complex at El Mirador, the largest building complex previously known for the Maya lowlands[7] (Extended Data Fig. 9c). In addition, the estimate for the La Danta complex assumed that the underlying bedrock surface was flat. Because many large buildings in the Maya area were constructed on naturally elevated locations (as in the case of the main plateau of Aguada Fénix, and the group A plateau of Ceibal), this figure for the La Danta complex may be an overestimate. It is unlikely that the real volume of the main plateau of Aguada Fénix is smaller than that of the La Danta complex of El Mirador.

Extended Data Figure 9b lists estimates of labour investment, corresponding to different estimates of volume. Detailed methods of calculating the labour investment have been discussed in a previous publication[4]. Our study followed previous research by other scholars (including experimental work), and assumed that the plateau of Aguada Fénix is made mostly of earth[24,71–73]. For the procurement of construction materials, we used a value of 2.6 $m^3$ of earth dug by one person a day[71]. For the transport of materials, we used an average transport distance of 500 m and assumed that a worker carried 500 kg or 0.384 $m^3$ of earth a day[71]. Plateau fills contained small iron and manganese oxide nodules, which suggests that they were taken from redoximorphic soils located nearby[74]. We think that the reservoirs found west of the plateau were originally burrows that were the result of the extraction of construction material. In addition, builders possibly invested some labour in the construction of fills beyond simply dumping transported earth. However, except for the fills with coloured clays, labour investments in the construction of most fills appear to have been small. To avoid an overestimation of labour investment, we did not include labour for fill construction. Such an estimate of labour investment may have a substantial margin of error. Our purpose is to give a general idea about how many builders could have participated, and to begin to think about the social processes associated with the construction of the plateau.

**Radiocarbon dating**

The 69 radiocarbon samples from Aguada Fénix and La Carmelita were analysed at the University of Tokyo Radiocarbon Dating laboratory (Supplementary Table 1). Most samples were treated with the acid–alkali–acid method, but three samples with low carbon contents (TKA-21334, TKA-21339 and TKA-21344) were treated with acid only. In addition, three more samples (TKA-21330, TKA-21336 and TKA-21337) had carbon contents lower than 10%. These six samples appear to have consisted mainly of soil organic matter rather than wood charcoal, and gave dates older than other samples. Those radiocarbon dates were treated as anomalous dates.

We conducted the Bayesian analysis of radiocarbon dates using the OxCal 4.3 program and the IntCal13 calibration curve[75–78]. For studies in the Maya region, some scholars recommend mixing IntCal

(which primarily represents conditions in the northern hemisphere), with SHCal (which represents the southern hemisphere)[79,80]. However, we do not have sufficient data to understand atmospheric mixing in the region, and we decided to use IntCal13 alone, which is based on higher-quality calibration data. In addition, chronologies of many Mesoamerican sites are based on IntCal, and the use of IntCal thus facilitates chronological comparisons between different regions of Mesoamerica.

Methods of Bayesian analysis have been discussed in detail[68,81–85]: here we present a brief summary. Bayesian analysis serves to refine radiocarbon dates by incorporating stratigraphic information and other archaeological data. It also estimates the beginning and end dates for an occupation phase. Moreover, Bayesian analysis helps to identify problematic dates through the visual representation of probability distributions and statistical measures (agreement indices and outlier models). These problematic dates are excluded from subsequent Bayesian models as outliers. For a radiocarbon date with an agreement index below 60%, we need to consider the possibility that it is an outlier. Whereas agreement indices facilitate the manual rejection of outliers, outlier models statistically identify probable outliers[86]. In examining radiocarbon dates from our excavations, we made separate Bayesian models for individual operations, incorporating information on stratigraphic sequences as a prior (Supplementary Methods). Because we are in the process of building a ceramic chronology for this region, we did not incorporate ceramic sequences in the Bayesian models.

In our primary Bayesian model (model 1), we manually rejected outliers, considering contextual information and agreement indices. At Aguada Fénix and other Mesoamerican sites, problematic dates often result from the recycling of old construction materials and the stratigraphic redeposition of old construction fills. In these cases, carbon samples give radiocarbon dates older than the dates of their final depositions. Stratigraphic mixing of younger carbons through animal burrows and root growths can occur, but such cases are less frequent. Thus, when inconsistencies among stratigraphically related radiocarbon dates existed, we usually assumed that radiocarbon dates older than expected dates were outliers. In addition to model 1, we created an outlier model (model 2). The results of the two models are generally consistent, which confirms the robustness of the models. Extended Data Figure 7 presents the main results of model 1, and the complete results of model 1 are shown in Supplementary Data and Supplementary Table 1.

Six radiocarbon dates from the deposit found in operation NR3A suggest that the use of ceramics at this site started around 1250 BC (1300–1130 BC at 95.4% level). The sequence of operation NR3A also indicates that the construction of the main plateau started around 1050 BC (1130–980 BC). Bayesian model 1 gives a slightly later date for the beginning of construction at operation NR7A (1070–925 BC), but this may be because of the small number of radiocarbon dates from this excavation. Although we favour the date around 1050 BC as a conservative estimate for the beginning of plateau construction, there remains the possibility that the construction started earlier. It is not clear whether the earliest deposits found on bedrock in operations NR3A and NR7A represent middens or construction fills. These deposits contained considerable quantities of partial ceramic vessels, large sherds, shells and bones, mixed in sticky black clay. Layers of similar black clay—although with lower densities of artefacts—were found on bedrock in other excavation units across the main plateau. Although we tentatively think that the earliest deposits in operations NR3A and NR7A were placed before the initial construction of the plateau, the nature of these layers should be further investigated.

In addition, the beginning of construction in the area around the E group is not clear. Sample TKA-20670, taken from the lowest layer (under floor 23) of operation NR5A in the E-group plaza, yielded one of the earliest dates at Aguada Fénix (1385–1135 BC). For now, we tentatively assume that this context represents occupation before plateau construction or a natural soil layer. In operation NR8A (placed to the west of the E group), we did not reach bedrock. Samples TKA-21370 and TKA-21371, collected from floor 19 of this excavation, returned modelled dates of 1090–980 BC and 1095–980 BC; Bayesian model 1 gives an estimate of 1965–945 BC for the beginning of the sequence at this location. With the currently available data, we cannot determine whether TKA-21370 and TKA-21371 resulted from old wood. Thus, there is the possibility that the area around the E group was constructed earlier than the southern and northern portions of the main plateau (thus, before 1050 BC). This possibility needs to be examined with more excavations.

### Reporting summary

Further information on research design is available in the Nature Research Reporting Summary linked to this paper.

## Data availability

The results of field investigations and laboratory analyses are described more in detail in annual reports presented to the Instituto Nacional de Antropología e Historia. Those reports, as well as the 3D models for volume calculation, are available at the University of Arizona Campus Repository (https://repository.arizona.edu/handle/10150/635527).

## Code availability

The OxCal code used for Bayesian analysis is provided in the Supplementary Information.


38. Chase, A. F. et al. Airborne LiDAR, archaeology, and the ancient Maya landscape at Caracol, Belize. *J. Archaeol. Sci.* **38**, 387–398 (2011).
39. Chase, A. F., Chase, D. Z., Fisher, C. T., Leisz, S. J. & Weishampel, J. F. Geospatial revolution and remote sensing LiDAR in Mesoamerican archaeology. *Proc. Natl Acad. Sci. USA* **109**, 12916–12921 (2012).
40. Chase, A. F. et al. Ancient Maya regional settlement and inter-site analysis: the 2013 west-central Belize LiDAR survey. *Adv. Archaeol. Pract.* **6**, 8671–8695 (2014).
41. Rosenswig, R. M., López-Torrijos, R., Antonelli, C. E. & Mendelsohn, R. R. Lidar mapping and surface survey of the Izapa state on the tropical piedmont of Chiapas, Mexico. *J. Archaeol. Sci.* **40**, 1493–1507 (2013).
42. Rosenswig, R. M. & López-Torrijos, R. Lidar reveals the entire kingdom of Izapa during the first millennium BC. *Antiquity* **92**, 1292–1309 (2018).
43. Hutson, S. R., Kidder, B., Lamb, C., Vallejo-Cáliz, D. & Welch, J. Small buildings and small budgets: making lidar work in northern Yucatan, Mexico. *Adv. Archaeol. Pract.* **4**, 268–283 (2016).
44. Reese-Taylor, K. et al. Boots on the ground at Yaxnohcah: ground-truthing lidar in a complex tropical landscape. *Adv. Archaeol. Pract.* **4**, 314–338 (2016).
45. Loughlin, M. L., Pool, C. A., Fernandez-Diaz, J. C. & Shrestha, R. L. Mapping the Tres Zapotes Polity: the effectiveness of lidar in tropical alluvial settings. *Adv. Archaeol. Pract.* **4**, 301–313 (2016).
46. Magnoni, A. et al. Detection thresholds of archaeological features in airborne lidar data from central Yucatán. *Adv. Archaeol. Pract.* **4**, 232–248 (2016).
47. Inomata, T. et al. Archaeological application of airborne LiDAR to examine social changes in the Ceibal region of the Maya lowlands. *PLoS ONE* **13**, e0191619 (2018).
48. Canuto, M. A. et al. Ancient lowland Maya complexity as revealed by airborne laser scanning of northern Guatemala. *Science* **361**, eaau0137 (2018).
49. Beach, T. et al. Ancient Maya wetland fields revealed under tropical forest canopy from laser scanning and multiproxy evidence. *Proc. Natl Acad. Sci. USA* **116**, 21469–21477 (2019).
50. Evans, D. H. et al. Uncovering archaeological landscapes at Angkor using lidar. *Proc. Natl Acad. Sci. USA* **110**, 12595–12600 (2013).
51. Evans, D. Airborne laser scanning as a method for exploring long-term socio-ecological dynamics in Cambodia. *J. Archaeol. Sci.* **74**, 164–175 (2016).
52. Fernandez-Diaz, J. C. et al. Capability assessment and performance metrics for the Titan multispectral mapping lidar. *Remote Sens.* **8**, 936 (2016).
53. Fernandez-Diaz, J. C., Carter, W. E., Shrestha, R. L. & Glennie, C. L. Now you see it … now you don't: understanding airborne mapping LiDAR collection and data product generation for archaeological research in Mesoamerica. *Remote Sens.* **6**, 9951–10001 (2014).
54. Hutson, S. R. Adapting LiDAR data for regional variation in the tropics: a case study from the Northern Maya lowlands. *J. Archaeol. Sci.* **4**, 252–263 (2015).
55. Prufer, K. M., Thompson, A. E. & Kennett, D. J. Evaluating airborne LiDAR for detecting settlements and modified landscapes in disturbed tropical environments at Uxbenká, Belize. *J. Archaeol. Sci.* **57**, 1–13 (2015).
56. Inomata, T. et al. Archaeological application of airborne LiDAR with object-based vegetation classification and visualization techniques at the lowland Maya site of Ceibal, Guatemala. *Remote Sens.* **9**, 563 (2017).
57. Venter, M. L., Shields, C. R. & Ordóñez, M. D. C. Mapping Matacanela: the complementary work of LiDAR and topographical survey in southern Veracruz, Mexico. *Anc. Mesoam.* **29**, 81–92 (2018).

58. Bennett, R., Welham, K. & Ford, A. A comparison of visualization techniques for models created from airborne laser scanned data. *Archaeol. Prospect*. **19**, 41–48 (2012).
59. Challis, K., Forlin, P. & Kincey, M. A generic toolkit for the visualization of archaeological features on airborne LiDAR elevation data. *Archaeol. Prospect*. **18**, 279–289 (2011).
60. Devereux, B. J., Amable, G. S. & Crow, P. Visualisation of LiDAR terrain models for archaeological feature detection. *Antiquity* **82**, 470 (2008).
61. Harmon, J. M., Leone, M. P., Prince, S. D. & Snyder, M. Lidar for archaeological landscape analysis: a case study of two eighteenth-century Maryland plantation sites. *Am. Antiq*. **71**, 649–670 (2006).
62. Millard, K., Burke, C., Stiff, D. & Redden, A. Detection of a low-relief 18th-century British siege trench using LiDAR vegetation penetration capabilities at Fort Beauséjour–Fort Cumberland National Historic Site, Canada. *Geoarchaeology* **24**, 576–588 (2009).
63. Štular, B., Kokalj, Ž., Oštir, K. & Nuninger, L. Visualization of lidar-derived relief models for detection of archaeological features. *J. Archaeol. Sci*. **39**, 3354–3360 (2012).
64. Chiba, T., Kaneta, S. & Suzuki, Y. Red relief image map: new visualization method for three dimensional data. *Int. Arch. Photogramm. Remote Sens. Spat. Inf. Sci* **37**, 1071–1076 (2008).
65. Chiba, T. & Suzuki, Y. Visualization of airborne laser mapping data: production and development of red relief image map. *Adv. Survey Technol. (in Japanese)* **96**, 32–42 (2008).
66. Inomata, T., Triadan, D. & Aoyama, K. After 40 years: revisiting Ceibal to investigate the origins of lowland Maya civilization. *Anc. Mesoam*. **28**, 187–201 (2017).
67. Sabloff, J. A. *Excavations at Seibal, Department of Peten, Guatemala: Ceramics* (Harvard Univ., 1975).
68. Inomata, T. et al. High-precision radiocarbon dating of political collapse and dynastic origins at the Maya site of Ceibal, Guatemala. *Proc. Natl Acad. Sci. USA* **114**, 1293–1298 (2017).
69. Inomata, T. The emergence of standardized spatial plans in southern Mesoamerica: chronology and interregional interactions viewed from Ceibal, Guatemala. *Anc. Mesoam*. **28**, 329–355 (2017).
70. Cyphers, A. & Murtha, T. in *Mesoamerican Plazas: Arenas of Community and Power* (eds Tsukamoto, K. & Inomata, T.) 71-89 (Univ. Arizona Press, 2014).
71. Erasmus, C. J. Monument building: some field experiments. *Southwest. J. Anthropol*. **21**, 277–301 (1965).
72. Abrams, E. M. *How the Maya Built their World: Energetics and Ancient Architecture* (Univ. Texas Press, 1994).
73. Ortmann, A. L. & Kidder, T. R. Building mound A at Poverty Point, Louisiana: monumental public architecture, ritual practice, and implications for hunter-gatherer complexity. *Geoarchaeology* **28**, 66–86 (2013).
74. Beach, T. et al. Stability and instability on Maya lowlands tropical hillslope soils. *Geomorphology* **305**, 185–208 (2018).
75. Bronk Ramsey, C. Radiocarbon calibration and analysis of stratigraphy: the OxCal program. *Radiocarbon* **37**, 425–430 (1995).
76. Bronk Ramsey, C. Bayesian analysis of radiocarbon dates. *Radiocarbon* **51**, 337–360 (2009).
77. Bronk Ramsey, C. *OxCal 4.3*. http://c14.arch.ox.ac.uk/ (2019).
78. Reimer, P. J. et al. IntCal13 and Marine13 radiocarbon age calibration curves 0–50,000 years cal bp. *Radiocarbon* **55**, 1869–1887 (2013).
79. Kennett, D. J. et al. Correlating the ancient Maya and modern European calendars with high-precision AMS $^{14}$C dating. *Sci. Rep*. **3**, 1597 (2013).
80. Hogg, A. G. et al. SHCal13 Southern Hemisphere calibration, 0–50,000 years cal BP. *Radiocarbon* **55**, 1889–1903 (2013).
81. Inomata, T., Ortiz, R., Arroyo, B. & Robinson, E. J. Chronological revisions of Preclassic Kaminaljuyú, Guatemala: implications for social processes in the southern Maya area. *Lat. Am. Antiq*. **25**, 377–408 (2014).
82. Buck, C. E., Kenworthy, J. B., Litton, C. D. & Smith, A. F. M. Combining archaeological and radiocarbon information: a Bayesian approach to calibration. *Antiquity* **65**, 808–821 (1991).
83. Buck, C. E., Cavanagh, W. G. & Litton, C. D. *Bayesian Approach to Interpreting Archaeological Data* (Wiley, 1996).
84. Bayliss, A. Rolling out revolution: using radiocarbon dating in archaeology. *Radiocarbon* **51**, 123–147 (2009).
85. Bayliss, A. Quality in Bayesian chronological models in archaeology. *World Archaeol*. **47**, 677–700 (2015).
86. Bronk Ramsey, C. Dealing with outliers and offsets in radiocarbon dating. *Radiocarbon* **51**, 1023–1045 (2009).
87. Coe, W. R. (ed). *Tikal Report No. 14: Excavations in the Great Plaza, North Terrace and North Acropolis of Tikal* (Univ. Museum, Univ. Pennsylvania, 1990).
88. Millon, R. The beginnings of Teotihuacan. *Am. Antiq*. **26**, 1–10 (1960).
89. Marquina, I. *Proyecto Cholula* (Instituto Nacional de Antropología e Historia, 1970).



**Acknowledgements** The permit for our research was granted by the Instituto Nacional de Antropología e Historia. Funding was provided by the Alphawood Foundation, the National Science Foundation (BCS-1826909), the Agnese Nelms Haury Program of the University of Arizona and JSPS KAKENHI (26101003). We thank R. Liendo, K. Teranishi, F. Kupprat, V. Poston, A. Flores, F. Pinzón, M. Mollinedo, C. Alvarado, H. Zanotto, D. Ramírez, S. Mendoza and O. García for their dedicated work.


**Author contributions** T.I. and D.T. designed the research. T.I., D.T., M.B.M.B., V.A.V.L. and M.G.H. conducted field investigations. T.I. planned the lidar survey, and J.C.F.-D. coordinated the acquisition and processing of high-resolution lidar data. T.I. analysed lidar data and made 3D bedrock models. H.N. analysed botanical remains, and T.O. conducted radiocarbon analysis. T.I. and T.O. carried out the Bayesian analysis of radiocarbon dates. T.B. conducted soil studies, and C.C. analysed starch grains. K.A. analysed obsidian artefacts. T.I. wrote the manuscript with input from others.

**Competing interests** The authors declare no competing interests.

**Additional information**


**Supplementary information** is available for this paper at https://doi.org/10.1038/s41586-020-2343-4.



**Correspondence and requests for materials** should be addressed to T.I.

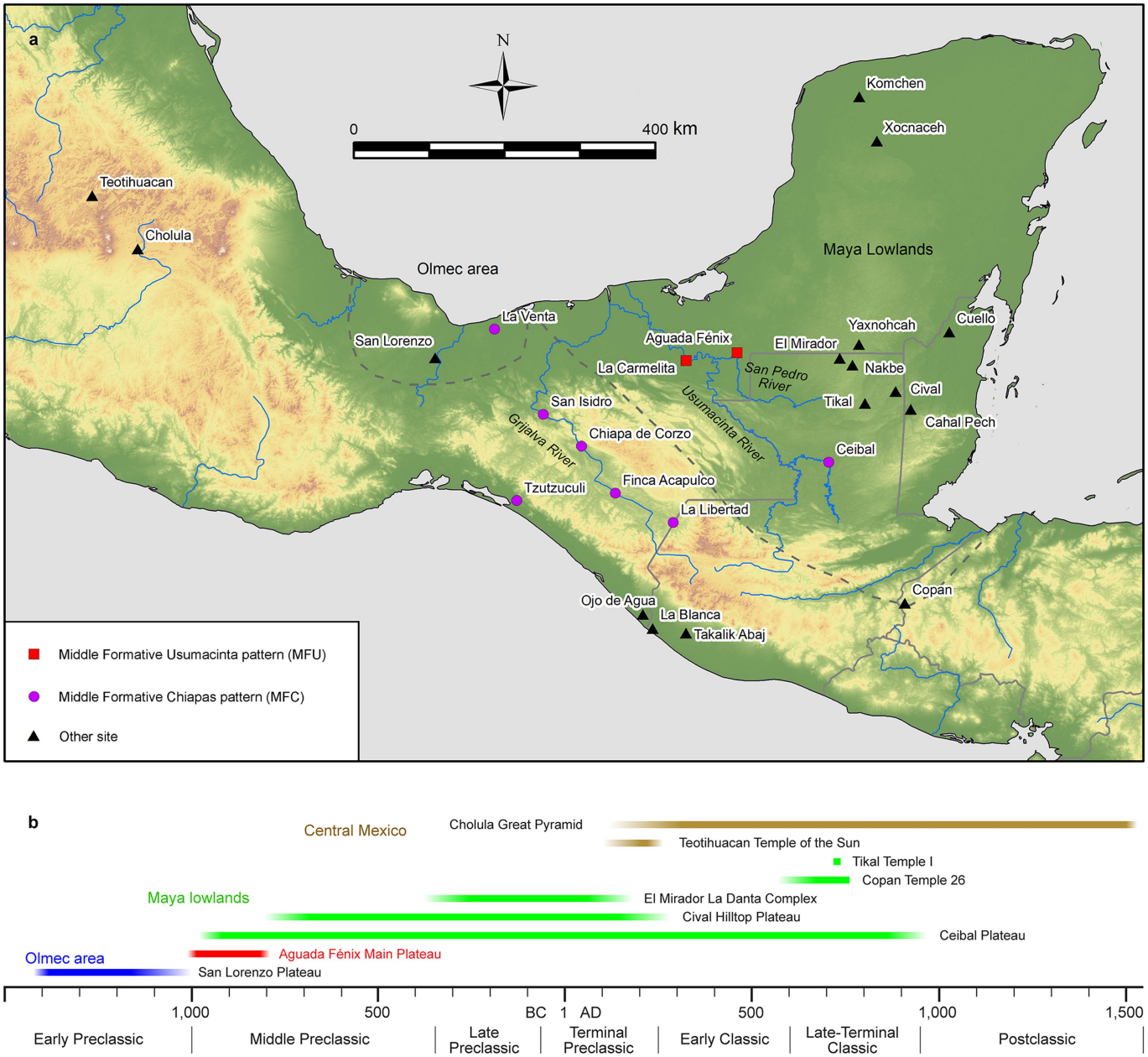


**Extended Data Fig. 1 | Geographical and chronological contexts of the study. a**, Map of Mesoamerica, showing the locations of the sites mentioned in the text. Map topographic data from the NASA-JPL Shuttle Radar Topographic Mission (https://www2.jpl.nasa.gov/srtm/). **b**, Chronology of Mesoamerica, indicating the construction dates of the Aguada Fénix main plateau and other major buildings listed in Extended Data Fig. 9c. Each bar shows the period in which a large portion of the building was constructed. Minor renovations and additions occurred outside of the indicated ranges.

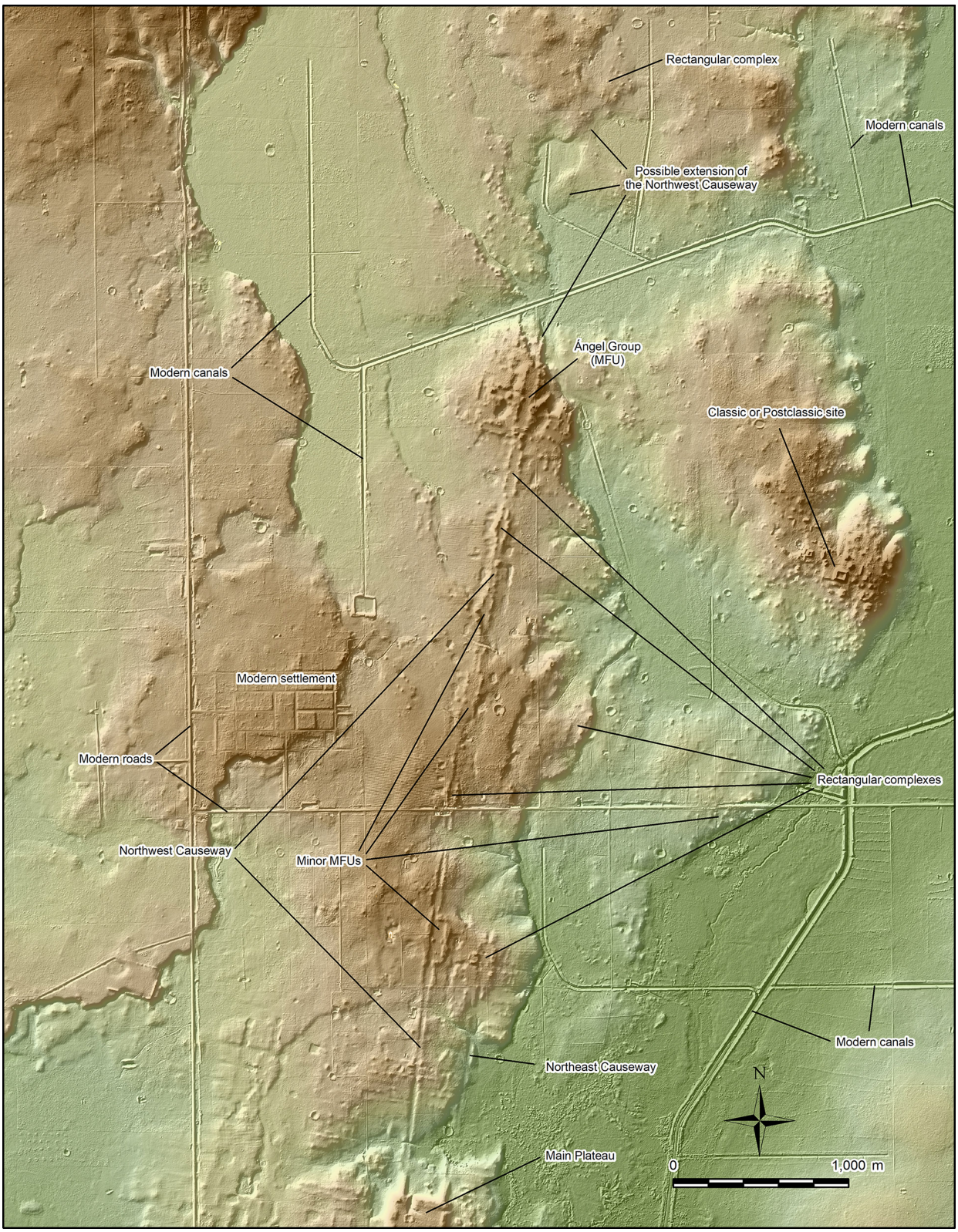


**Extended Data Fig. 2 | High-resolution lidar image of the north causeways of Aguada Fénix.** The causeways are connected to the main plateau by large ramps. The northwest causeway is the longest at the site, and connects multiple MFU complexes and rectangular complexes along the way.

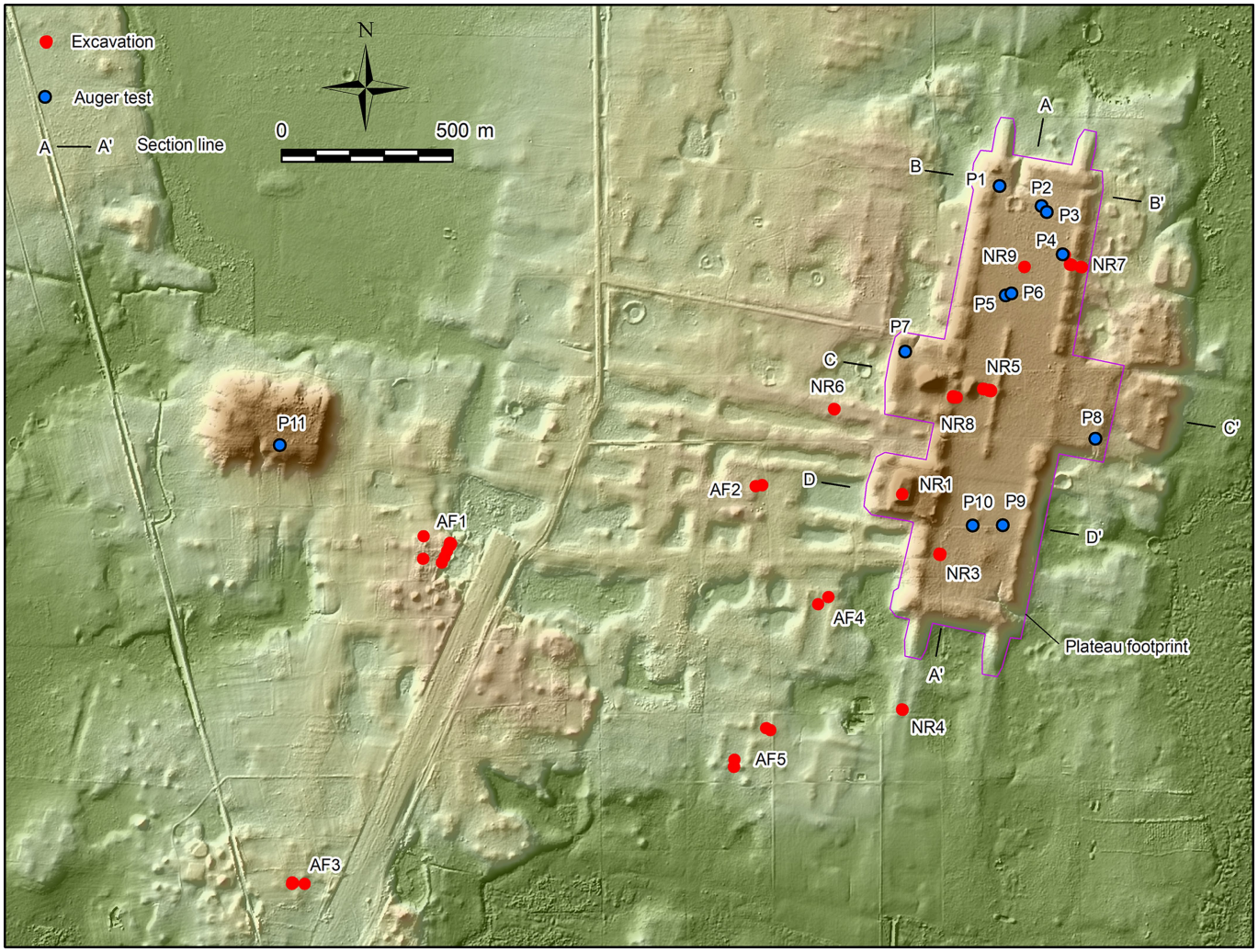


**Extended Data Fig. 3 | Locations of excavations and auger tests at Aguada Fénix.** The footprint of the main plateau indicated in this figure was used for the calculations of plateau fill volumes. The locations of the section drawings shown in Extended Data Fig. 9 are also indicated.

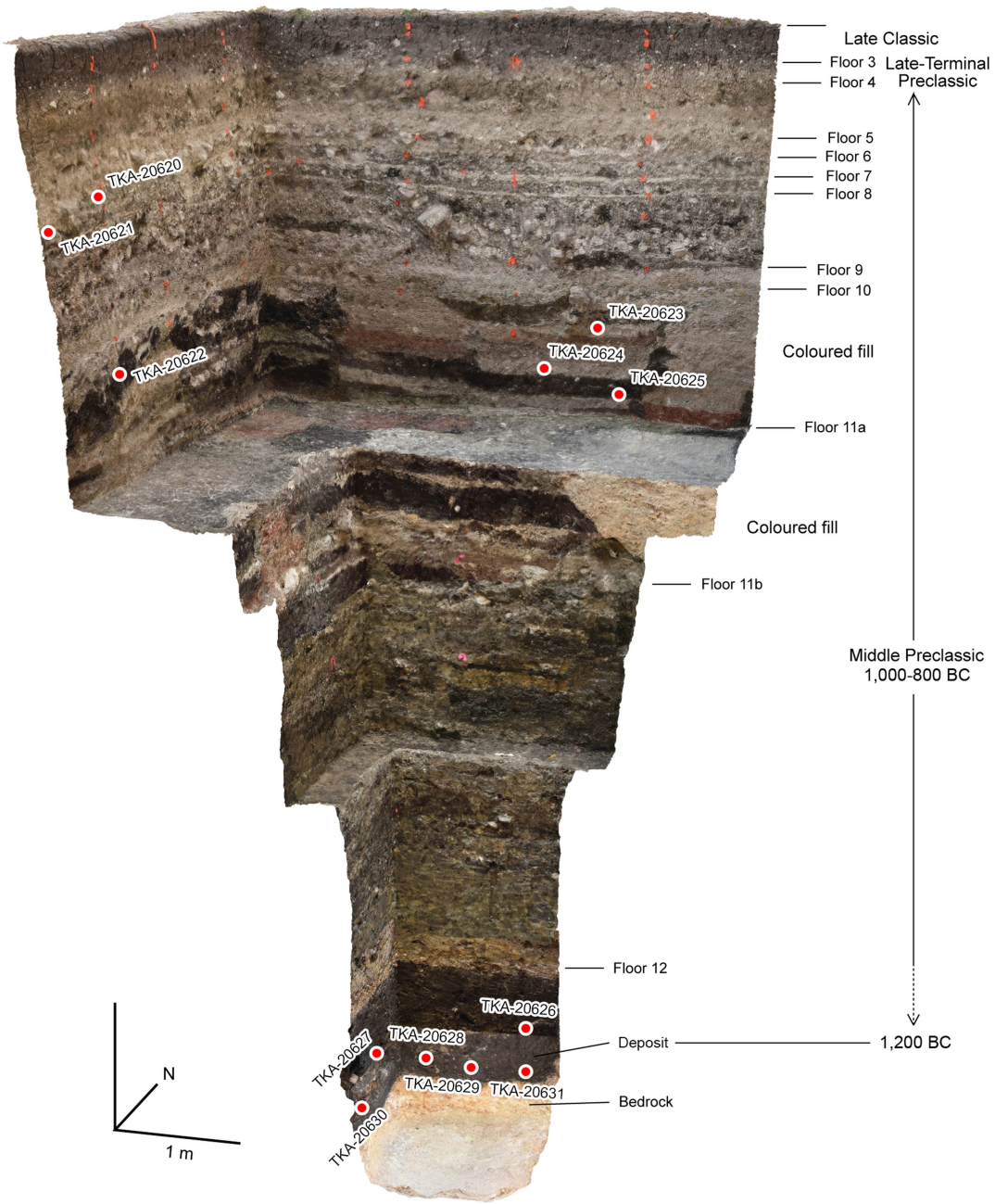


**Extended Data Fig. 4 | Composite 3D photogrammetry image of operation NR3, showing the north and east profiles.** The locations of radiocarbon samples are projected to the nearest profiles. The image shows that a substantial part of the plateau fills was placed during the period between 1000 and 800 BC. The fills between floors 10 and 11b consist of clays and other soils of multiple colours in checkerboard-like patterns.


**Extended Data Fig. 5 | Construction fills with clays and other soils of multiple colours found in operation NR3 (a 4 × 4-m excavation, viewed from the south). a**, Upper layer directly under floor 10. **b**, Middle layer. **c**, Lower layer. Blocks of soils in different colours are separated by dividers made of black clay and other soils. **d**, North profile. This sequence shows that blocks of soils in different colours were placed in multiple layers above floor 11a in one construction event. They were covered by floor 10 at the end of the sequence.


**Extended Data Fig. 6 | Megalithic structure found in operation NR8.** **a**, Composite 3D photogrammetry image of the structure and the excavation. **b**, Back wall viewed from the interior (from the southwest). **c**, Back wall viewed from the exterior (from the east) (2-m-wide trench). There was a deposit of broken ceramics placed at the end of the Late Classic period. **d**, Back terrace retaining wall, viewed from the east (2-m-wide trench).

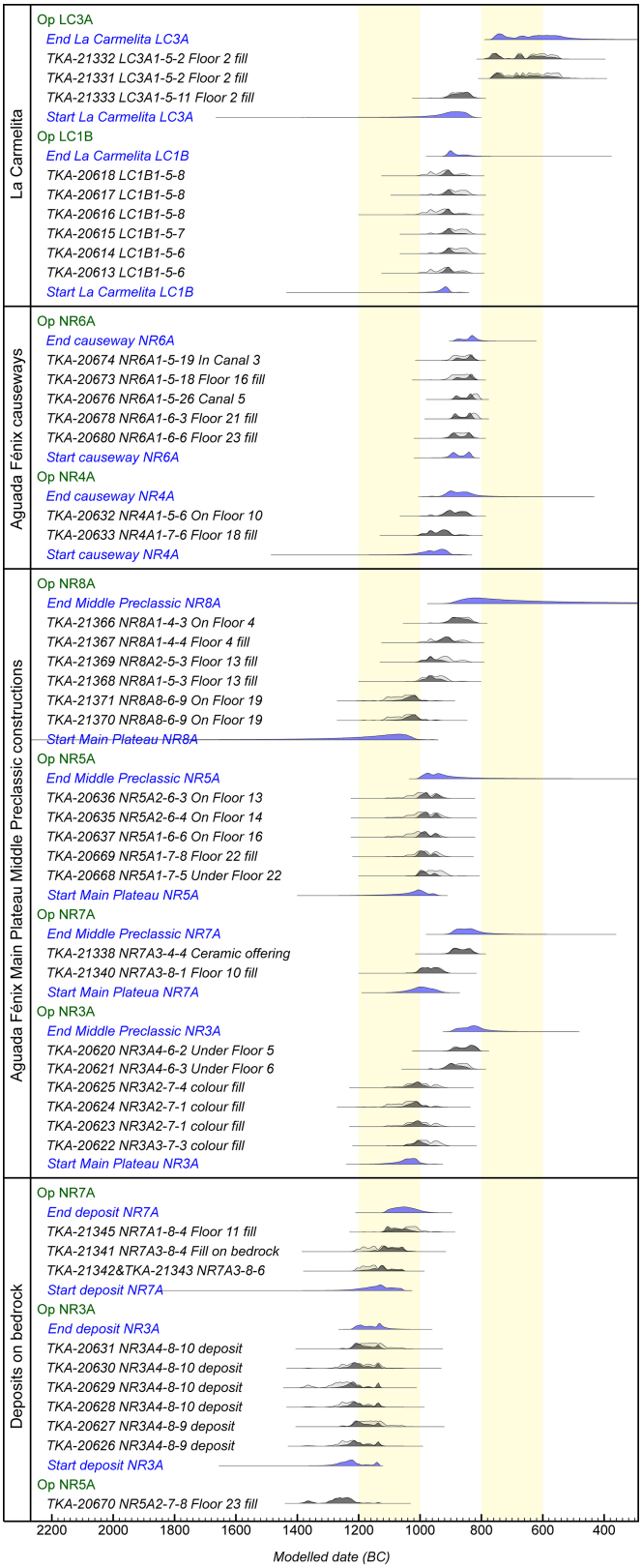


**Extended Data Fig. 7 | Radiocarbon dates from Aguada Fénix and La Carmelita.** Radiocarbon dates for the Middle Preclassic period and key boundary dates are shown, excluding outliers. Black areas indicate the probability distributions of modelled dates obtained with model 1, and grey areas show those of unmodelled calibrated dates. Dates in blue represent boundary dates. The entire OxCal results of model 1 are provided in Supplementary Table 1 and Supplementary Data.

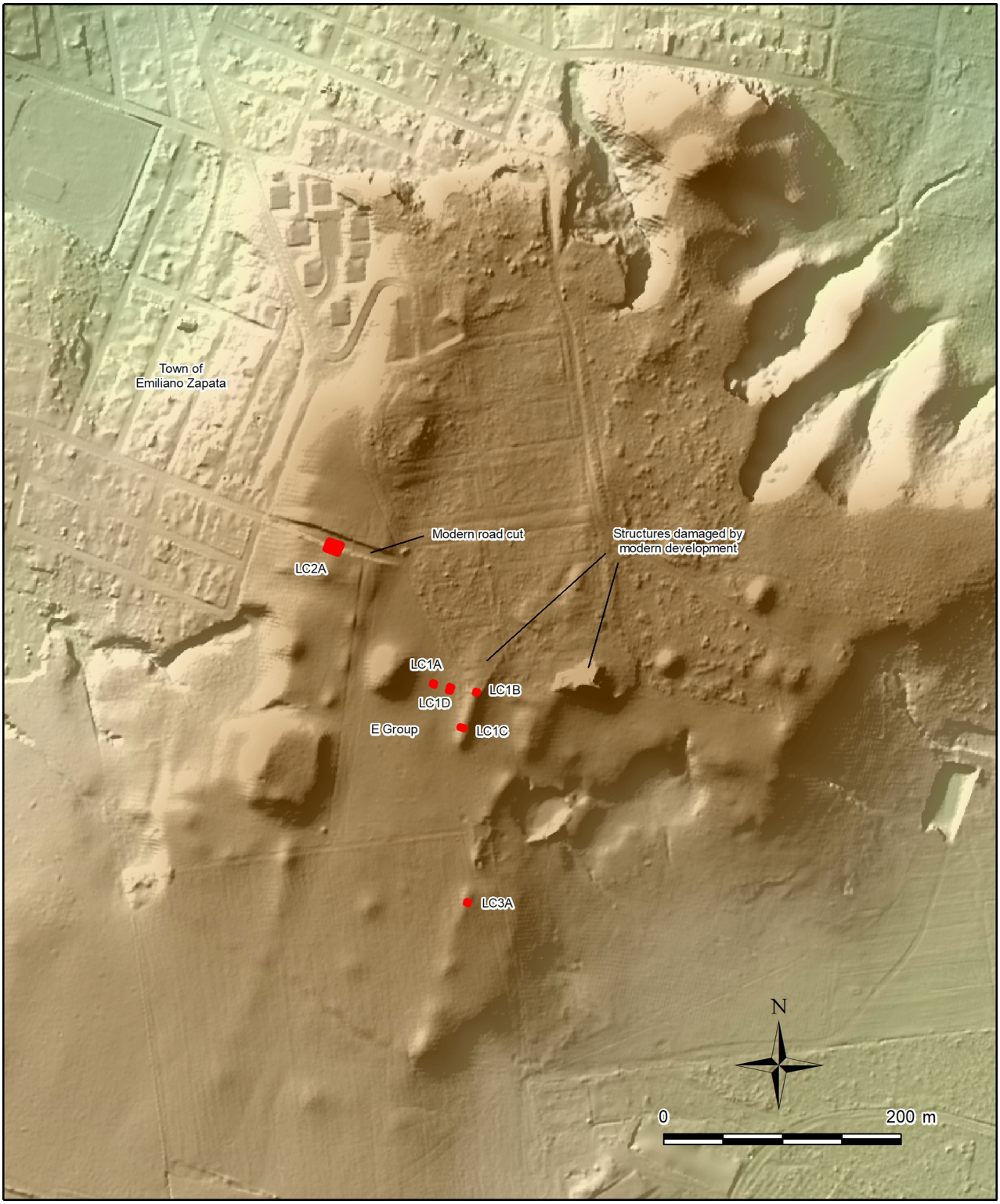


**Extended Data Fig. 8 | Locations of excavations at La Carmelita.** The northern part of the site, including the northern portion of the eastern platform of the E group, was damaged by a modern development project. The construction was halted by the Mexican government after initial destruction.

**a**

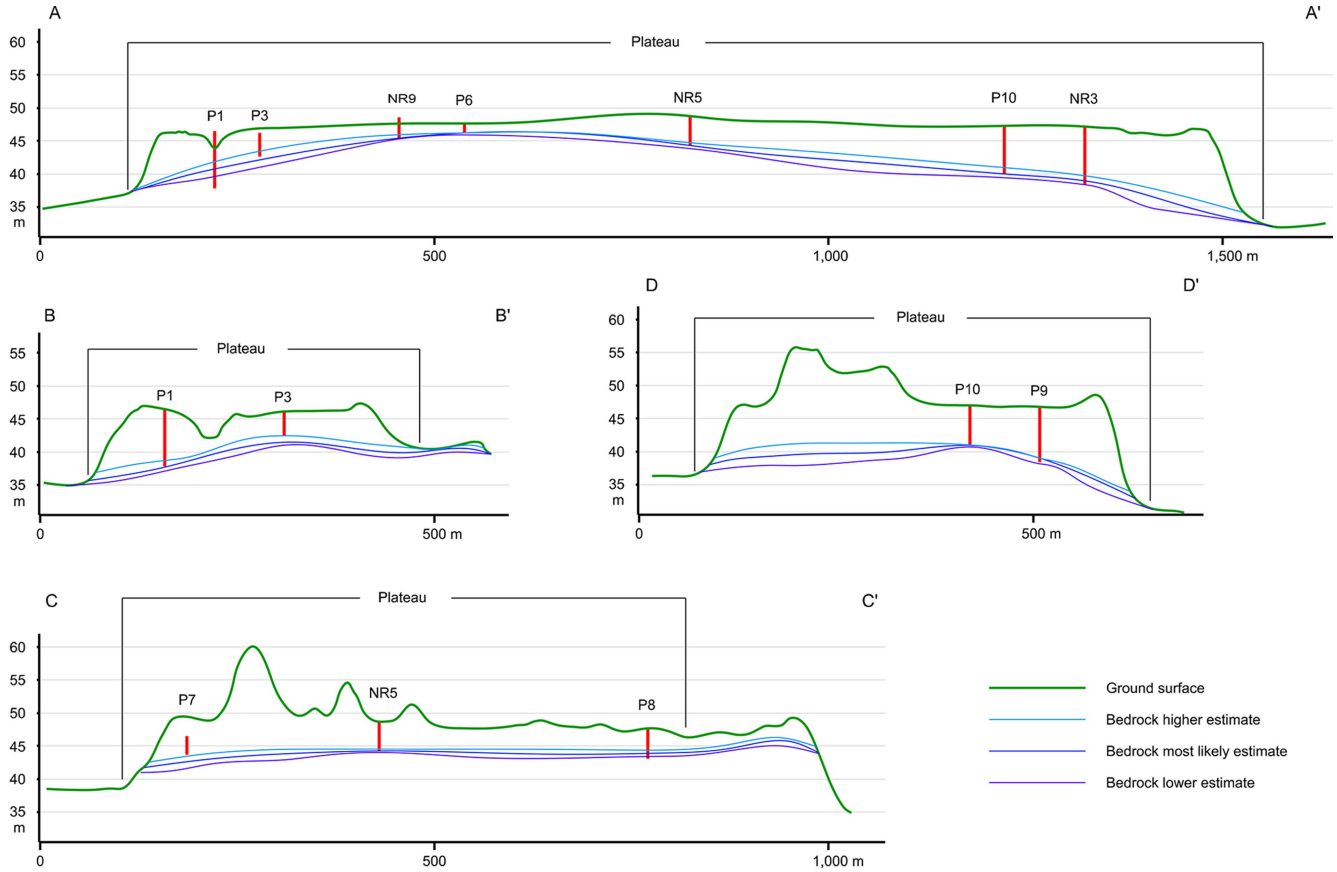


**b**

| Aguada Fénix structure | Estimate | Volume ($m^3$) | Labor investment (person-day) |
|---|---|---|---|
| Main Plateau all periods | High | 4,480,000 | 13,400,000 |
| | Most likely | 3,790,000 | 11,300,000 |
| | Low | 3,390,000 | 10,100,000 |
| Main Plateau Middle Preclassic | High | 4,320,000 | 12,900,000 |
| | Most likely | 3,630,000 | 10,800,000 |
| | Low | 3,230,000 | 9,700,000 |
| West Plateau Middle Preclassic | High | 1,150,000 | 3,400,000 |
| | Low | 610,000 | 1,800,000 |
| Combined Middle Preclassic | High | 5,470,000 | 16,300,000 |
| | Low | 3,840,000 | 11,500,000 |

**c**

| Site | Structure | Volume ($m^3$) | Period | Reference |
|---|---|---|---|---|
| Aguada Fénix | Main Plateau | 3,200,000-4,300,000 | Middle Preclassic (1,000-800 BC) | |
| | West Plateau | 600,000-1,200,000 | Middle Preclassic | |
| | Combined | 3,800,000-5,500,000 | Middle Preclassic | |
| Ceibal | Group A Plateau | 710,000 | Preclassic to Classic | 4 |
| Cival | Hilltop plateau | 1,900,000 | Preclassic | 5 |
| El Mirador | La Danta Complex | 2,800,000 | Mostly Late to Terminal Preclassic | 7 |
| | El Tigre Complex | 430,000 | Mostly Late to Terminal Preclassic | 7 |
| | Combined | 3,200,000 | Mostly Late to Terminal Preclassic | 7 |
| Tikal | Temple I | 18,300 | Late Classic | 24,87 |
| Copan | Temple 26 | 31,900 | Mostly Late Classic | 24 |
| San Lorenzo | Plateau | 6,000,000-8,000,000 | Early Preclassic | 13 |
| Teotihuacan | Pyramid of the Sun | 1,600,000 | Terminal Preclassic | 88 |
| | Pyramid of the Moon | 320,000 | Terminal Preclassic to Early Classic | 88 |
| | Combined | 1,900,000 | Terminal Preclassic to Early Classic | 88 |
| Cholula | Great Pyramid | 4,500,000 | Preclassic to Postclassic | 89 |

**Extended Data Fig. 9 | Calculation of the volume of the main plateau at Aguada Fénix. a**, Section drawings of the plateau, showing the current ground surface and the estimated positions of bedrock. Vertical dimensions are exaggerated. The locations of the section lines are shown in Extended Data Fig. 3. Red lines indicate the depths of bedrock reached by excavations and auger tests. When excavations and auger tests are not on the section lines, their elevations may not correspond exactly with the positions of the current ground surface and bedrock shown here. **b**, Estimated construction volumes of the main plateau and the west plateau of Aguada Fénix, and estimates of labour investment. **c**, Comparison of the Aguada Fénix plateaus with other major buildings[4,5,7,13,24,87–89] in Mesoamerica. The construction volume of the main plateau of Aguada Fénix is larger than that of the La Danta complex (the largest construction in the Maya lowlands previously known) and that of the Pyramid of the Sun of Teotihuacan, the largest city in Preclassic-to-Classic Mesoamerica. The Great Pyramid of Cholula is larger, but it was expanded over more than 1,000 years.


**Extended Data Fig. 10 | Early Middle Preclassic caches found at Aguada Fénix. a**, **b**, Cache NR3 (found in operation NR5B), which was placed on the east–west axis of the E-group plaza. It contained six axes and a perforator (all made of greenstone), as well as three small pieces of greenstone. The pointed end of the perforator is broken. The contents and location of this cache closely resemble those found at San Isidro, Chiapa de Corzo, Ceibal and Cival. Similar caches of greenstone axes were also found at La Venta, although not in the E-group plaza. These deposits, along with the similarities in site layout, show that these Middle Preclassic centres shared spatial and ritual concepts. **c**–**e**, Cache AF1, found in operation AF1D. It contained a limestone sculpture—possibly representing a white-lipped peccary—that we named 'Choco'. The naturalistic image of an animal contrasts with Olmec art, which depicts supernatural beings and high-status individuals.

nature research

Corresponding author(s): Takeshi Inomata

Last updated by author(s): Apr 6, 2020

# Reporting Summary

Nature Research wishes to improve the reproducibility of the work that we publish. This form provides structure for consistency and transparency in reporting. For further information on Nature Research policies, see Authors & Referees and the Editorial Policy Checklist.

## Statistics

For all statistical analyses, confirm that the following items are present in the figure legend, table legend, main text, or Methods section.

| n/a | Confirmed |
|---|---|
| ☐ | ☒ The exact sample size (*n*) for each experimental group/condition, given as a discrete number and unit of measurement |
| ☐ | ☒ A statement on whether measurements were taken from distinct samples or whether the same sample was measured repeatedly |
| ☐ | ☒ The statistical test(s) used AND whether they are one- or two-sided<br>*Only common tests should be described solely by name; describe more complex techniques in the Methods section.* |
| ☒ | ☐ A description of all covariates tested |
| ☒ | ☐ A description of any assumptions or corrections, such as tests of normality and adjustment for multiple comparisons |
| ☒ | ☐ A full description of the statistical parameters including central tendency (e.g. means) or other basic estimates (e.g. regression coefficient) AND variation (e.g. standard deviation) or associated estimates of uncertainty (e.g. confidence intervals) |
| ☒ | ☐ For null hypothesis testing, the test statistic (e.g. *F*, *t*, *r*) with confidence intervals, effect sizes, degrees of freedom and *P* value noted<br>*Give P values as exact values whenever suitable.* |
| ☐ | ☒ For Bayesian analysis, information on the choice of priors and Markov chain Monte Carlo settings |
| ☒ | ☐ For hierarchical and complex designs, identification of the appropriate level for tests and full reporting of outcomes |
| ☒ | ☐ Estimates of effect sizes (e.g. Cohen's *d*, Pearson's *r*), indicating how they were calculated |

*Our web collection on statistics for biologists contains articles on many of the points above.*

## Software and code

Policy information about availability of computer code

| | |
|---|---|
| Data collection | Lidar data acquisition and processing were done with Optech LMS 4.4.0, Terrasolid TerraScan 019.003 and Golden Software Surfer 12. |
| Data analysis | Lidar-derived DEMs were analyzed with ESRI ArcGIS 10.7.1.<br>The production of a 3D model of bedrock and fill volume calculation were done with ArcGIS and Bentley Microstation 08.11.09.829.<br>The composite phogrammetry image of excavation (Extended Data Figure 4) was made with Agisoft PhotoScan 1.4.4.<br>The Bayesian analysis of radiocarbon dates was done with Oxcal 4.3.<br>The Oxcal codes for this analysis are included as Supplementary Information. |

For manuscripts utilizing custom algorithms or software that are central to the research but not yet described in published literature, software must be made available to editors/reviewers. We strongly encourage code deposition in a community repository (e.g. GitHub). See the Nature Research guidelines for submitting code & software for further information.

## Data

Policy information about availability of data

All manuscripts must include a data availability statement. This statement should provide the following information, where applicable:

- Accession codes, unique identifiers, or web links for publicly available datasets
- A list of figures that have associated raw data
- A description of any restrictions on data availability

The results of field investigations and lab analyses are described more in detail in the annual reports presented to the Instituto Nacional de Antropología e Historia. Those reports, as well as the 3D models for volume calculation, are available at the University of Arizona Campus Repository (https://repository.arizona.edu/arizona/).

# Field-specific reporting

Please select the one below that is the best fit for your research. If you are not sure, read the appropriate sections before making your selection.

☐ Life sciences ☒ Behavioural & social sciences ☐ Ecological, evolutionary & environmental sciences

For a reference copy of the document with all sections, see nature.com/documents/nr-reporting-summary-flat.pdf

# Behavioural & social sciences study design

All studies must disclose on these points even when the disclosure is negative.

| | |
|---|---|
| Study description | This is an archaeological study of past society, including excavations, surveys, lidar, artifact analysis and radiocarbon dating. It involves quantitative data on structures sizes and radiocarbon dates, as well as the qualitative study of social processes. |
| Research sample | The research sample consists of archaeological data obtained from lidar, ground surveys, excavations, artifact analysis and radiocarbon dates. We used existing low-resolution lidar data, which were made publicly avaible by the INEGI (www.inegi.org.mx) and covers the entire study area. We selected the areas for high-resolution lidar, where important sites were found in the INEGI lidar. At Aguada Fénix, we selected 5 excavation areas on the plateau, 2 areas on causeways, and 5 areas in the periphery to examine construction history across the site. At La Carmelita, we selected 5 excavation areas to examine the construction history of this smaller site. We chose sixty nine radiocarbon dates to date the entire the entire occupation history of Aguada Fénix and La Carmelita. |
| Sampling strategy | No sample size calculation was performed. The high-resolution lidar covers the entire sites of Aguada Fénix and La Carmelita. The locations of excavations and auger tests were selected to cover different parts of the sites. Thus, the excavation samples are representative of the construction volume and occupation history. The excavations at La Carmelita provide representative data to reconstruction the construction history of its ceremonial core. Sixty nine radiocarbon dates cover the entire occupation sequences and are representative. |
| Data collection | The high-resolution lidar data were collected with Optech Titan lidar. Excavation data were recorded on paper forms in the field and then input in computer files. Photographs of excavations were taken with Nikon D750 and D7000 digital cameras.<br>In addition to the authors of this paper, other archaeologists, archaeology students, and local community members participated in excavations. |
| Timing | Archaeological fieldwork was conducted July-August 2017, February-April 2018, February-April 2019 and February-March 2020. High-resolution lidar data were collected in May 2017 and June 2019. |
| Data exclusions | No excavation data were excluded. In the Bayesian analysis of radiocarbon dates, we followed the pre-established and commonly accepted criteria for exclusion (agreement indices lower than about 60 and the results of outlier models). Fourteen dates were excluded as outliers from the models. |
| Non-participation | The study does not involve participants. |
| Randomization | Locations for excavations and lidar surveys were not randomized. As the lidar covers the entire sites and excavations targeted different parts of the sites, they provided necessary data for the reconstruction of construction sequences and fill volumes. |

# Reporting for specific materials, systems and methods

We require information from authors about some types of materials, experimental systems and methods used in many studies. Here, indicate whether each material, system or method listed is relevant to your study. If you are not sure if a list item applies to your research, read the appropriate section before selecting a response.

## Materials & experimental systems

| n/a | Involved in the study |
|---|---|
| ☒ | ☐ Antibodies |
| ☒ | ☐ Eukaryotic cell lines |
| ☒ | ☐ Palaeontology |
| ☒ | ☐ Animals and other organisms |
| ☒ | ☐ Human research participants |
| ☒ | ☐ Clinical data |

## Methods

| n/a | Involved in the study |
|---|---|
| ☒ | ☐ ChIP-seq |
| ☒ | ☐ Flow cytometry |
| ☒ | ☐ MRI-based neuroimaging |